Prediction of Rashba Effect on Two-dimensional MX Monochalcogenides (M = Ge, Sn and X = S, Se, Te) with Buckled Square Lattice

Ibnu Jihad*, Juhri Hendrawan, Adam Sukma Putra, Kuwat Triyana, and Moh. Adhib Ulil Absor

*Department of Physics, Faculty of Mathematics and Natural Sciences, Universitas Gadjah Mada,
Sekip Utara BLS 21, Yogyakarta 55281, Indonesia*

Abstract: *The Rashba splitting are found in the buckled square lattice. Here, by applying fully relativistic density-functional theory (DFT) calculation, we confirm the existence of the Rashba splitting in the conduction band minimum of various two-dimensional MX monochalcogenides (M = Ge, Sn and X = S, Se, Te) exhibiting a pair inplane Rashba rotation of the spin textures. A strong correlation has also been found between the size of the Rashba parameter and the atomic number of chalcogen atom for Γ and M point in the first Brillouin zone. Our investigation clarifies that the buckled square lattice are promising for inducing the substantial Rashba splitting suggesting that the present system is promising for spintronics device.*

Keywords: *Ge monochalcogenides; Sn monochalcogenides; DFT method; spintronics; square lattice; Rashba effect; spin textures*

■ INTRODUCTION

Spintronics is a combinational word from spin transport electronics or spin electronics, which is the next generation of electronics. Spintronics explores the spin properties of electrons rather than the charge properties in electronics device, in which give us more degree of freedom [1]. This fact makes spintronics device have higher information density and also energetically efficient because the smaller movement is needed for changing (reading and writing) the spin structure. One branch of the spintronics research field is spin-orbitronics, which is focused on the exploitation of non-equilibrium material properties using spin-orbit coupling (SOC). In the spin-orbitronics, the investigation is aiming for searching materials that have large enough SOC energy splitting, especially the Rashba effect type to build spin field-effect transistor (SFET) [2].

The Rashba splitting in the electronics band structures is caused by the lack of inversion symmetry of the materials [3], which occurred in a two-dimensional (2D) structures of materials. Graphene as the first example of the 2D materials having hexagonal structure have been considered for this purpose. However, due to the weak SOC, this material is not suitable for spin-orbitronics [4-6]. Another example of 2D materials having hexagonal structure is coming from the transition metal dichalcogenides (TMDs) family [7]. Here, the breaking of inversion symmetry in the hexagonal crystal, together with the strong SOC of transition metal atom leads to the strong SOC splitting. Recently, the 2D Group-IV monochalcogenides in square lattice with black phosphorus structure have been recently studied and proved as a suitable semiconductor with sizeable Rashba splitting [9].

Although the SOC has been widely studied on the 2D materials with the hexagonal structure and black phosphorus structure, this effect should apparently appear on the other non-centrosymmetric 2D materials. One of the candidates is 2D material which posses a square lattice structure. The square lattice structure with buckling has also been experimentally observed on Bismuth (Bi) [10], making the realization of this structure is plausible. Computational research on buckled square lattice of lead chalcogenides showing significant first-order Rashba effect in this structure [8]. Previously, a preliminary study on the electronic structure of the MX monochalcogenides (M = Ge, Sn

and X = S, Se) has been conducted with buckled squared lattice and also the calculation of Rashba splitting size up to the-third order correction that was showing a sizeable Rashba splitting in these materials [9].

This work showed that the Rashba splitting is also observed in the MTe monochalcogenides (M = Ge, Sn) with buckled squared lattice as additional materials to MX monochalcogenides (M = Ge, Sn and X = S, Se) buckled square lattice. It is found that the substantial Rashba splitting is achieved in the conduction band minimum of various 2D MX monochalcogenides showing clockwise-anticlockwise rotation of the spin in the momentum space. From these various TMDs materials, the size of the Rashba parameter is strongly affected by the atomic number of chalcogen atoms for different high symmetry points in the first Brillouin zone.

COMPUTATIONAL METHOD

This work was started by modeling the two-dimensional monolayer buckled square lattice crystal (Fig. 1). The distance between slabs is set to 30 Å to prevent interaction between slabs. The coordinate axis is x = a, y = b, and c = z. The geometry is relaxed until the force of each atom less than 1 meV/Å.

The calculation was performed using a density functional theory (DFT) approach implemented on OPENMX code [10] within the generalized gradient approximation (GGA) for the exchange-correlation energy [11]. The norm-conserving pseudopotentials [12] was set to energy cut off 300 rydberg for charge density. The optimum k-point sampling for the calculation is 8 × 8 × 1. The wave function was expanded by a confinement scheme of a linear combination of multiple pseudoatomic orbitals [13-14]. The numerical pseudoatomic orbitals

used for M atom was two-s, two-p, three-d, and one-f, and for X atom was three-s, three-p, two-d, and one-f. The j-dependent pseudopotentials were applied for SOC [15]. After gaining the stable structure of the materials, the process continue to calculate the electronics band structures with the corresponding density of states (DOS) projected to the atomic orbitals.

RESULTS AND DISCUSSION

The optimized structure and the related parameters, are summarized in Table 1 and have good agreement with previous report [9]. The PbS and PbSe calculations have been presented to confirm the computational results with previously reported data [8].

The result of the electronic band structures is displayed in Fig. 2. It is observed that in the calculation without including SOC (blue lines in band structure), the valence band maximum (VBM) located in Y (and X') point for all MX. While In conduction band, the extremum valley or the conduction band minimum occurred along the Y-M line, for all MX. This result has a similarity with the previous result of MX with black phosphorene lattice structure. However, in black phosphorene, the different band structure was observed [16]. Our calculated DOS projected to the atomic orbitals confirmed that the VBM is dominated by a mixture of X-p_z and M-p_z. The CBM is contributed by the coupling of M-p_z and M-p_y. The band gap energy of all MX buckled square lattice monolayer has an indirect type. These calculated values are different from black phosphorene structure [9]. However, both structures have typical pattern in the band gap properties. The band gap are decreased along with the increasing chalcogen atomic mass in the buckles square lattice, thus
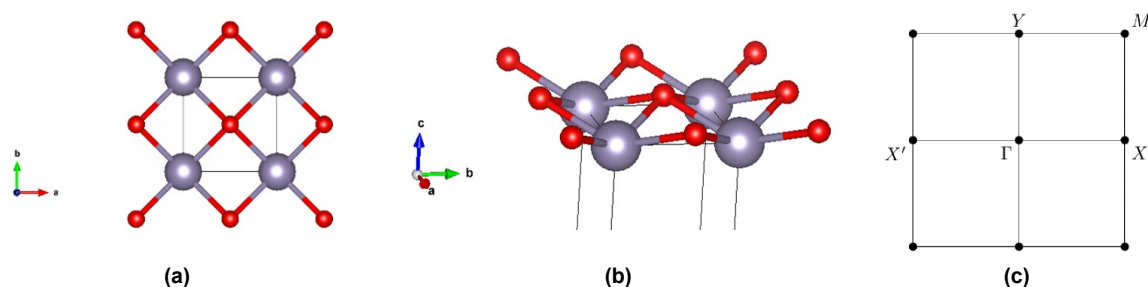
Fig 1. 2D buckled square lattice (drawing using Vesta) (a) from top and (b) side and (c) the first Brillouin zone

Table 1. Calculation result of lattice constant, buckling distance, and buckling angle

	Calculation			References			
	a(Å)	d_z(Å)	θ (°)	a(Å)	d_z(Å)	θ (°)	Source
PbS	3.76	1.04	21.4	3.76	1.0841	22.17	[8]
PBSe	3.79	1.27	25.4	3.85	1.2087	23.92	[8]
GeO	2.86	0.76	20.6	-	-	-	This work
GeS	3.25	1.14	26.4	3.31	1.10868	25.35	[9]
GeSe	3.42	1.22	26.8	3.46	1.18338	25.83	[16]
GeTe	3.69	1.30	26.5	-	-	-	This work
SnO	3.16	0.76	18.8	-	-	-	This work
SnS	3.54	1.20	25.6	3.55	1.18601	25.32	[16]
SnSe	3.62	1.34	27.6	3.68	1.27148	26.07	[16]
SnTe	3.94	1.41	26.8	-	-	-	This work
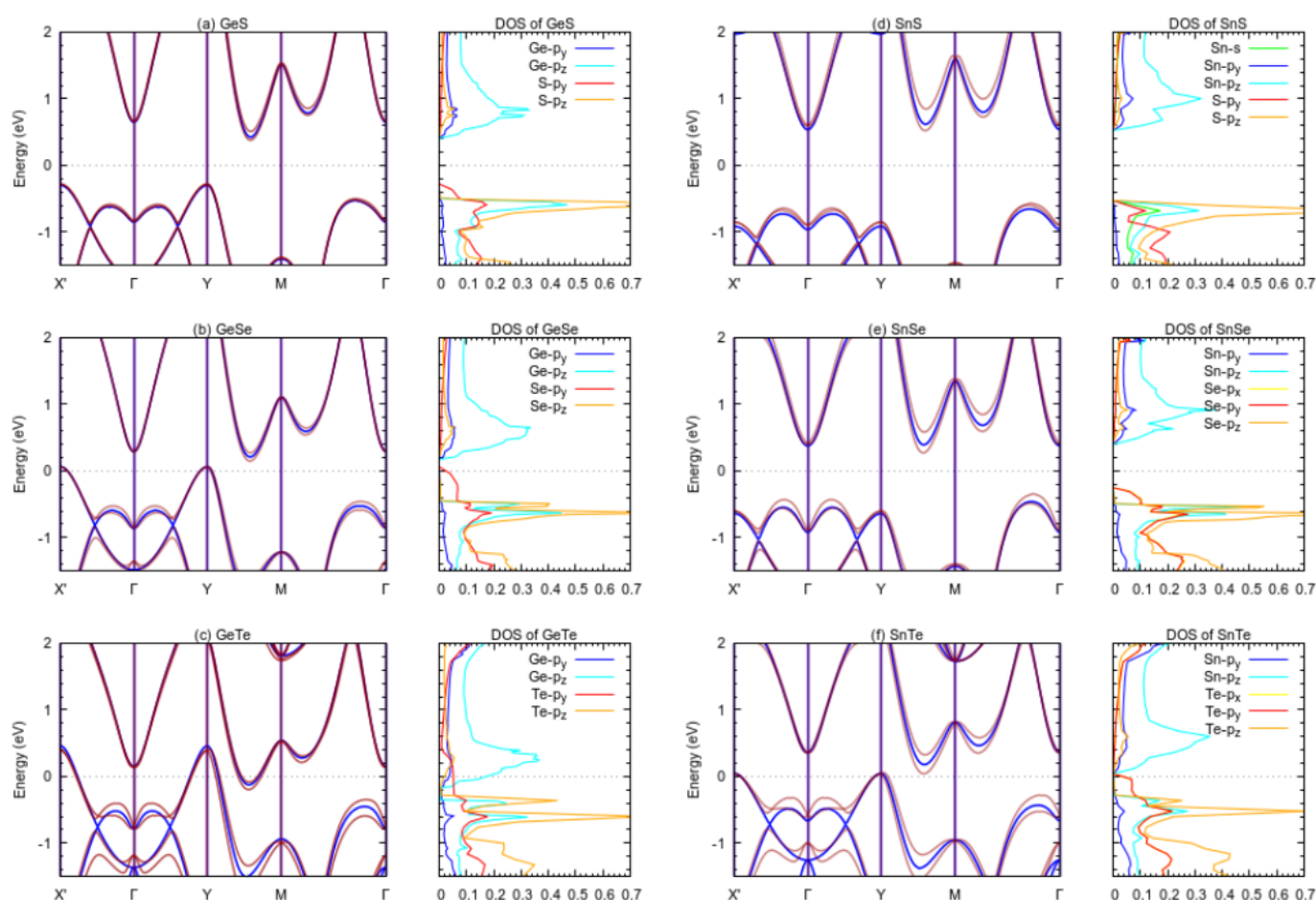
Fig 2. The Brillouin zone in k-space of the square lattice structure. Blue and pink line indicating the energy band without SOC and with SOC, respectively. The dominant DOS is displayed with corresponding orbitals

resulting in a lower band gap [17-19]. The band gap values are GeS = 0.660 eV, GeSe = 0.085 eV, GeTe = no band gap, SnSe = 1.097 eV, SnSe = 0.627 eV, and SnTe = no bandgap. From this band gap, all of MX is semiconductor except GeTe and SnTe, which is metallic.

When the calculation includes the SOC term, all of the bands are split due to the lack of inversion symmetry, which is occurs in all MX. The clarification of the

occurrence of the spin-split states is by considering the characteristic of the atomic orbitals of the band. From atomic point of view, coupling between atomic orbitals will contribute to the non-zero SOC matrix element through the relation $\zeta_l \langle \vec{L} \cdot \vec{S} \rangle_{u,v}$, where ζ_l is the angular-momentum-resolved atomic SOC strength, with $l = (s, p, d)$, $\vec{L}$ and $\vec{S}$ are the orbital angular momentum and Pauli spin operator, respectively, for the (u, v) atomic orbitals. It is revealed that the dominant contribution in CBM is coming from coupling between p orbitals of M atom and p orbitals of chalcogen atom for all MX. This p-p coupling is enhanced by increasing the atomic number of chalcogen atom. This finding is consistent with the enhancement of the spin splitting size around the Γ point. The more detailed discussion about the quantitative size of the splitting will be presented later.

Next, the spin-splitting near Γ and M-points of the CBM is claimed as Rashba-type splitting because the spin orientation is rotational [3], and we will show the calculation of this spin orientation (which is known as spin textures). It is well-known that there are three kinds

of SOC splitting in non-centrosymmetric and non-magnetic materials, namely Rashba, Dresselhaus, and Zeeman-like splitting [20], where the spin splitting and their corresponding spin textures are displayed in Fig. 3. The figure shows that the Rashba and Dresselhaus splitting is very similar except for the spin textures.

Next, the calculation of the size of the Rashba splitting in the buckled MX square lattice materials and the spin textures is conducted to clarify the claim that this is an actual Rashba splitting. To calculate the size of Rashba splitting (Rashba parameter) for higher-order, first is to use symmetry analysis to derive the effective Hamiltonian via k.p perturbation approximation. This approximation allows us to describe the electronic properties of our 2D MX monochalcogenides and can be used to analyze the properties of the band structure, such as spin splitting and spin texture for points around VBM and CBM. This method has already successfully used in various 2D material [7,21-25]. The symmetry group of the 2D square lattice structure is isomorphic to the C_{2v} or 2 mm two-dimensional space group [26], and from
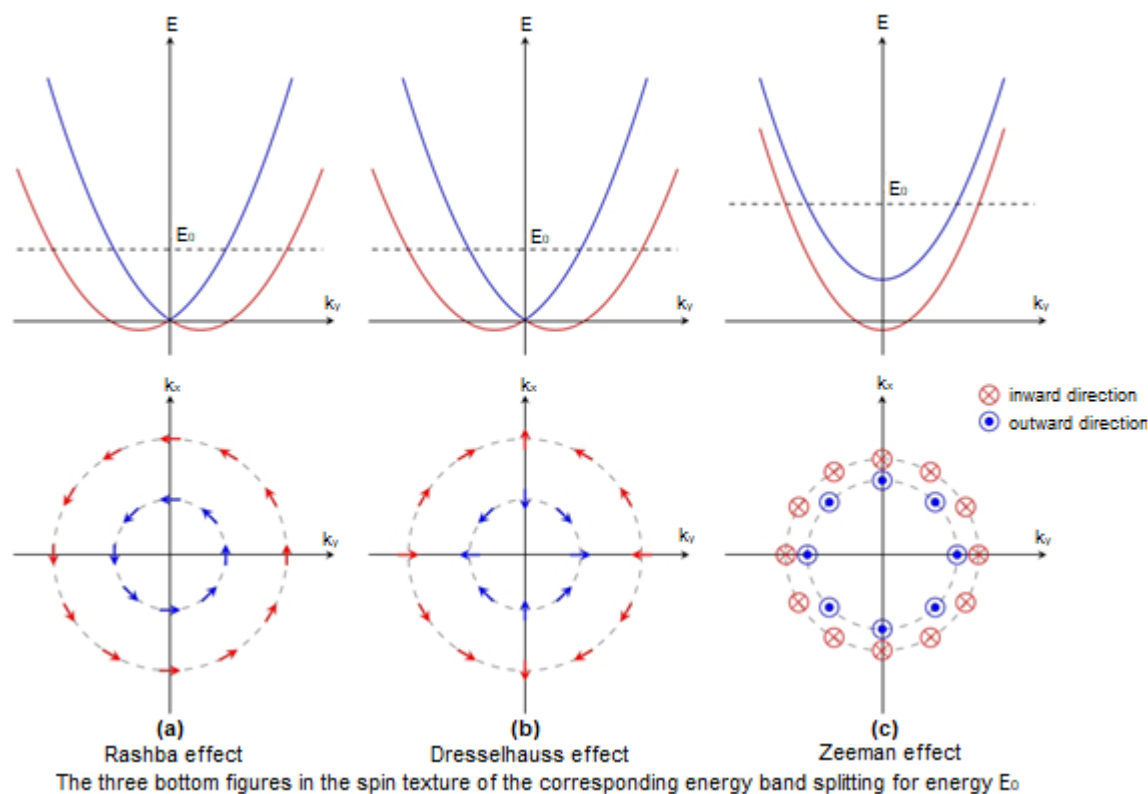

(a)
Rashba effect

(b)
Dresselhauss effect

(c)
Zeeman effect

The three bottom figures in the spin texture of the corresponding energy band splitting for energy E_0

Fig 3. Three kinds of SOC splitting with the spin orientation

previous analysis using group theory [24], by deriving the general Hamiltonian using the direct product of irreducible representations. The elements of the group are denoted by $E: \{x, y, z\}$, $C_2: \{-x, -y, z\}$, $T_x: \{-x, y, z\}$, and $T_y: \{x, -y, z\}$. This group has four one-dimensional irreducible representations, A_1, A_2, B_1, and B_2 with the character table is written in Table 2.

The corresponding component of the irreducible representation is set to the polar-vector k and the axial-vector σ for the first order combination that corresponds to the A_1 irreducible representation is $B_1: k_x, \sigma_y$, $B_2: k_y, \sigma_x$, and $A_2: \sigma_z$. For the second-order, $A_1: k_x^2, k_y^2, k_y^2$, and $A_2: k_x k_y$, which is this second-order implies the form of kinetic energy. Finally, the third-order term is the possible product of $B_1: k_x^3, k_x k_y^2$, and $B_2: k_y^3, k_y k_x^2$ with σ_i. Then a new total Hamiltonian, that leaves the old one invariant, is constructed to get the new Hamiltonian related to SOC up to third-order as:

$$H(k) = E_0(k) + \alpha_1^{(1)} k_x \sigma_y + \alpha_1^{(2)} k_y \sigma_x + \alpha_3^{(1)} k_x^3 \sigma_y + \alpha_3^{(2)} k_x^2 k_y \sigma_x + \alpha_3^{(3)} k_x k_y^2 \sigma_y + \alpha_3^{(4)} k_y^3 \sigma_x \quad (1)$$

where $E_0(k) = \hbar^2 \left(\frac{k_x^2}{2m_x^*} + \frac{k_y^2}{2m_y^*} \right)$ is the nearly free-electron energy, $\alpha_j^{(i)}$ is the i-th coefficient of the j-order, $\sigma_x, \sigma_y, \sigma_z$ is the Pauli spin matrices, (k_x, k_y) is the position in k-space and $k = \sqrt{k_x^2 + k_y^2}$. The eigenvalues problems for Eq. (1) gives us the splitting energy:

$$E_\pm(k, \theta) = E_0(k) \pm \sqrt{X^2 + Y^2} \quad (2)$$

with

$$Y = \alpha_1^{(2)} k\sin\theta + \alpha_3^{(2)} k^3 \cos^2\theta \sin\theta + \alpha_3^{(4)} k^3 \sin^3\theta$$
$$X = \alpha_1^{(1)} k\cos\theta + \alpha_3^{(1)} k^3 \cos^3\theta + \alpha_3^{(3)} k^3 \sin^2\theta\cos\theta$$

where $k_x = k\cos\theta$, $k_y = k\sin\theta$, and θ is the angle of k with x-axis in k-space. The eigenvectors related to the $\pm\sqrt{(X^2 + Y^2)}$ eigenvalues is

$$\psi_\pm(k) = \begin{pmatrix} 0 \\ \pm \frac{(Y+iX)}{\sqrt{X^2+Y^2}} \end{pmatrix} \quad (3)$$

The square of the difference of energy eigenvalue can be calculated using:

$$(\Delta E(k))^2 = 4(\alpha_1^{(1)} k_x + \alpha_3^{(1)} k_x^3 + \alpha_3^{(3)} k_x k_y^2)^2 + 4(\alpha_1^{(2)} k_y + \alpha_3^{(2)} k_x^2 k_y + \alpha_3^{(4)} k_y^3)^2 \quad (4)$$

This equation is used to fit the plot of $(\Delta E(k))^2$ along Γ-X and Y-M and get the non-vanishing first-order coefficient as the Rashba parameter. The fitting results for the Rashba parameter are displayed in Table 3 with PbS calculation is shown as a confirmation. The table shows that for Γ-point, the size of the Rashba parameter increases depending on the atomic number of chalcogen atom, while on the M-point, the parameter is decreased.

Next, the spin texture of the band structures is determined as follows. For a given k point, its spin polarization of each eigenstates $\psi_\pm(k)$ is define as $S(k) = [S_x(k), S_y(k), S_z(k)]$ where $S_i(k) = \frac{\hbar}{2} \langle \psi(k) | \sigma_i \psi(k) \rangle$ is

Table 2. Character table of C₂ᵥ group

	E	C_2	T_x	T_y
A_1	1	1	1	1
A_2	1	1	-1	-1
B_1	1	-1	-1	1
B_2	1	-1	1	-1

Table 3. Calculation result of band gap and Rashba parameter in CBM

MX	Band Gap (eV)	Fitting Result (eVÅ)		Reference (eVÅ)		Source
		Γ-point ($\alpha_1^{(1)}$)	M-point ($\alpha_1^{(2)}$)	Γ-point	M-point	
PbS	0.747	1.20	3.19	1.03	5.10	[8]
GeS	0.660	0.20	0.68	0.201	0.583	[9]
GeSe	0.085	0.27	0.52	0.320	0.468	[16]
GeTe	Conductor	0.38	0.34	-	-	This work
SnS	1.097	0.42	2.36	0.429	2.354	[16]
SnSe	0.627	0.58	1.48	0.548	1.746	[16]
SnTe	Conductor	0.59	1.05	-	-	This work
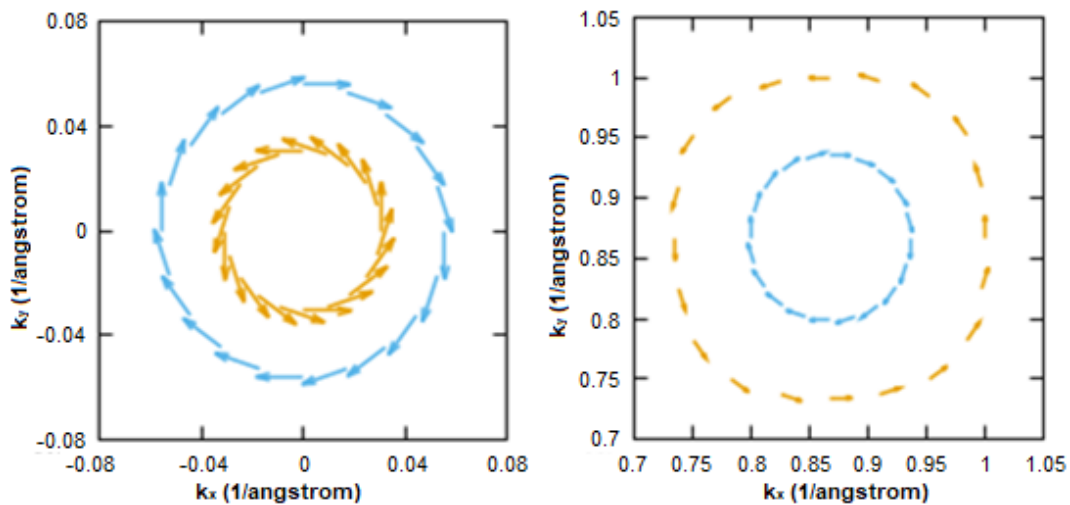
Fig 4. (left) Spin texture of SnTe for energy 0.4 eV around Γ-point, (right) Spin texture of SnSe for energy 1.15 eV around M-point. Both have zero z-component of spin. A similar form also occurred in other MX

the i-direction of spin component. This spin polarization is calculated in k-space around Γ point by using the spin density matrix of the spinor wave functions obtained from the DFT calculation [21-23]. The calculation result is shown in Fig. 4. It is revealed that constant-energy surface shows the inner and outer circles with counterclockwise and clockwise rotation of spin direction with no z-component of spin. This feature is consistent with the characteristic of the Rashba effect splitting.

The observed spin texture can be explained based on our derived SOC Hamiltonian given in Eq. (1). The expectation value of the spin polarization can be calculated from this to get $\langle S_x \rangle_{\pm} = \frac{\pm Y\hbar}{\sqrt{(X^2+Y^2)}}$, $\langle S_y \rangle_{\pm} = \frac{\pm X\hbar}{\sqrt{(X^2+Y^2)}}$, and $\langle S_z \rangle_{\pm} = 0$. This result shows that the spin textures are consistent with Fig. 4.

■ **CONCLUSION**

Investigation of the Rashba effect on two-dimensional MX Monochalcogenides (M = Ge, Sn and X = S, Se, Te) with buckled square lattice has shown that this structure is appropriate to create the Rasbha splitting. We also confirmed the properties of the spin texture of SOC splitting with the calculation from our DFT results. We found that some of MX have semiconductor properties (except GeTe and SnTe) and have different Rashba parameter. There is a strong correlation between the size of the Rashba parameter with the chalcogen atomic

number. In Γ-point, the escalation of the chalcogen atomic number increases the Rasha parameter, but in M-point the effect is inverting. These various size of the Rashba parameter make these materials, and this buckled square lattice is potential to be developed for spintronics materials.

■ **REFERENCES**

[1] Bhatti, S., Sbiaa, R., Hirohata, A., Ohno, H., Fukami, S., and Piramanayagam, S.N., 2017, Spintronics based random access memory: A review, *Mater. Today*, 20 (9), 530–548.

[2] Datta, S., and Das, B., 1990, Electronic analog of the electro-optic modulator, *Appl. Phys. Lett.*, 56 (7), 665–667.

[3] Manchon, A., Koo, H.C., Nitta, J., Frolov, S.M., and Duine, R.A., 2015, New perspectives for Rashba spin-orbit coupling, *Nat. Mater.*, 14 (9), 871–882.

[4] Tombros, N., Jozsa, C., Popinciuc, M., Jonkman, H.T., and van Wees, B.J., 2007, Electronic spin

transport and spin precession in single graphene layers at room temperature, *Nature*, 448 (7153), 571–574.

[5] Yan, W., Phillips, L.C., Barbone, M., Hämäläinen, S.J., Lombardo, A., Ghidini, M., Moya, X., Maccherozzi, F., van Dijken, S., Dhesi, S.S., Ferrari, A.C., and Mathur, N.D., 2016, Long spin diffusion length in few-layer graphene flakes, *Phys. Rev. Lett.*, 117 (14), 147201.

[6] Dlubak, B., Martin, M.B., Deranlot, C., Servet, B., Xavier, S., Mattana, R., Sprinkle, M., Berger, C., De Heer, W.A., Petroff, F., Anane, A., Seneor, P., and Fert, A., 2012, Highly efficient spin transport in epitaxial graphene on SiC, *Nat. Phys.*, 8 (7), 557–561.

[7] Absor, M.A.U., Santoso, I., Harsojo, Abraha, K., Kotaka, H., Ishii, F., and Saito, M., 2017, Polarity tuning of spin-orbit-induced spin splitting in two-dimensional transition metal dichalcogenides, *J. Appl. Phys.*, 122 (15), 153905.

[8] Hanakata, P.Z., Rodin, A.S., Carvalho, A., Park, H.S., Campbell, D.K., and Castro Neto, A.H., 2017, Two-dimensional square buckled Rashba lead chalcogenides, *Phys. Rev. B: Condens. Matter*, 96 (16), 161401.

[9] Hendrawan, J., Absor, M.A.U., Arifin, M., Jihad, I., and Abraha, K., 2019, Electronics structure of monochalcogenide materials MX (M = Ge, Sn and Pb; X = S and Se) buckled square lattice, *IOP Conf. Ser.: Mater. Sci. Eng.*, 515 (1), 012105.

[10] Ozaki, T., Kino, H., Yu, J., Han, M.J., Kobayashi, N., Ohfuti, M., Ishii, F., Ohwaki, T., Weng, H., and Terakura, K., 2009, *OpenMX: Open source package for Material eXplorer*, http://www.openmx-square.org/.

[11] Perdew, J.P., Burke, K., and Ernzerhof, M., 1996, Generalized gradient approximation made simple, *Phys. Rev. Lett.*, 77 (18), 3865–3868.

[12] Troullier, N., and Martins, J.L., 1991, Efficient pseudopotentials for plane-wave calculations, *Phys. Rev. B: Condens. Matter*, 43 (3), 1993–2006.

[13] Ozaki, T., 2003, Variationally optimized atomic orbitals for large-scale electronic structures, *Phys. Rev. B: Condens. Matter*, 67 (15), 155108.

[14] Ozaki, T., and Kino, H., 2004, Numerical atomic basis orbitals from H to Kr, *Phys. Rev. B: Condens. Matter*, 69 (19), 195113.

[15] Theurich, G., and Hill, N.A., 2001, Self-consistent treatment of spin-orbit coupling in solids using relativistic fully separable ab initio pseudopotentials, *Phys. Rev. B: Condens. Matter*, 64 (7), 073106.

[16] Absor, M.A.U., and Ishii, F., 2019, Intrinsic persistent spin helix state in two-dimensional group-IV monochalcogenide MX monolayers (M = Sn or Ge and X = S, Se or Te), *Phys. Rev. B: Condens. Matter*, 100 (11), 115104.

[17] Gomes, L.C., and Carvalho, A., 2015, Phosphorene analogues: Isoelectronic two-dimensional group-IV monochalcogenides with orthorhombic structure, *Phys. Rev. B: Condens. Matter*, 92 (8), 085406.

[18] Xu, L., Yang, M., Wang, S.J., and Feng, Y.P., 2017, Electronic and optical properties of the monolayer group-IV monochalcogenides MX (M = Ge, Sn; X = S, Se, Te), *Phys. Rev. B: Condens. Matter*, 95 (23), 235434.

[19] Wan, W., Liu, C., Xiao, W., and Yao, Y., 2017, Promising ferroelectricity in 2D group IV tellurides: A first-principles study, *Appl. Phys. Lett.*, 111 (13), 132904.

[20] Acosta, C.M., Fazzio, A., and Dalpian, G.M., 2019, Zeeman-type spin splitting in nonmagnetic three-dimensional compounds, *npj Quantum Mater.*, 4 (1), 41.

[21] Absor, M.A.U., Santoso, I, Harsojo, Abraha, K., Kotaka, H., Ishii, F., and Saito, M., 2018, Strong Rashba effect in the localized impurity states of halogen-doped monolayer PtSe2, *Phys. Rev. B: Condens. Matter*, 97 (20), 205138.

[22] Kotaka, H., Ishii, F., and Saito, M., 2013, Rashba effect on the structure of the Bi one-bilayer film: Fully relativistic first-principles calculation, *Jpn. J. Appl. Phys.*, 52 (3R), 035204.

[23] Absor, M.A.U., Kotaka, H., Ishii, F., and Saito, M., 2016, Strain-controlled spin splitting in the conduction band of monolayer WS2, *Phys. Rev. B: Condens. Matter*, 94 (11), 115131.

[24] Vajna, S., Simon, E., Szilva, A., Palotas, K., Ujfalussy, B., and Szunyogh, L., 2012, Higher-order contributions to the Rashba-Bychkov effect with application to the Bi/Ag(111) surface alloy, *Phys. Rev. B: Condens. Matter*, 85 (7), 075404.

[25] Affandi, Y., and Absor, M.A.U., 2019, Electric field-induced anisotropic Rashba splitting in two dimensional tungsten dichalcogenides WX_2 (X: S, Se, Te): A first-principles study, *Physica E*, 114, 113611.

[26] Dresselhaus, M.S., Dresselhaus, G., and Jorio, A., 2008, *Group Theory – Application to the Physics of Condensed Matter*, Springer-Verlag, Heidelberg, Germany.